Z. Physik B 24, 293–299 (1976)

Zeitschrift für Physik B

The Scattering of Phonons of Arbitrary Wavelength at a Solid-Solid Interface: Model Calculation and Applications

Ch. Steinbrüchel
The James Franck Institute, The University of Chicago, Chicago, Illinois, U.S.A.

Received March 16, 1976

A one-dimensional lattice model of a solid-solid interface is presented within which it is possible to characterize the scattering of phonons at the interface as a function of wavelength. The probability for a phonon to be transmitted across the interface is found generally to decrease with decreasing wavelength, although phenomena such as total reflexion and resonant transmission may occur. Conditions for the existence of a localized interface mode are given. The thermal boundary resistance for heat flow across the interface is expressed in terms of an average temperature-dependent phonon transmission coefficient which generally increases with decreasing temperature and approaches the continuum value at very low temperature. Applications of these results to three-dimensional interfaces in general, and particularly to heat dissipation in catalysts, high-frequency phonon radiators, and Kapitza resistance, are discussed.

1. Introduction

When heat is conducted from one material to another, for most practical purposes the temperature can be regarded as a continuous function across the interface. This is not a good approximation, however, in a number of situations of experimental interest. It has been known for some time that heat flow from a solid to liquid helium is accompanied by a finite temperature jump at the interface [1]. A similar effect can occur at the interface between two solids, at least one of which is an insulator, if a large heat flux is involved [2–5].

This phenomenon of thermal boundary resistance has been rationalized on the basis that heat is transmitted by phonons across the interface. The transmission probability for phonons is determined according to the so-called acoustic mismatch theory [6, 7], i.e. by calculating the transmission coefficient of an elastic wave impinging on the interface. This theory provides a qualitatively satisfactory description of heat transfer across a metal-insulator interface at low [8, 9] as well as at high temperature [3–5]. The situation is less clear in the case of an interface involving liquid helium. The theory appears to be adequate for temperatures below 0.1 K if allowance is made for phonon attenuation in the solid [1, 10, 11]. Above 0.1 K the theory predicts much too small a thermal boundary resistance. The mechanisms responsible for this surprisingly efficient heat transfer into liquid helium are still being investigated [1].

As indicated above, the acoustic mismatch theory is basically a continuum theory. Hence it should be expected to be valid only for long-wavelength phonons, i.e. only at low temperatures. Because of its continuum character, the acoustic mismatch theory completely neglects the structure of the interface on an atomic scale. However, this structure is clearly crucial in determining the scattering of phonons whose wavelength is comparable with the thickness of the interface, i.e. with the distance over which the elastic properties change appreciably.

In this paper, I shall present a simple one-dimensional lattice model of a solid-solid interface within which it is possible to investigate in some detail the effect of the atomic structure of the interface on the scattering of phonons. Specifically, I shall calculate the probability for a phonon to be transmitted across the interface as a function of wavelength. I shall also evaluate the heat flux due to phonons across the interface as a function of temperature, and I shall express this heat flux in terms of an average temperature-dependent transmission coefficient which will be the proper generalization of the continuum transmission coefficient to higher temperatures. Finally, I shall discuss the application of these results to three-dimensional interfaces in general, and particularly to heat dissipation in catalysts, to high-frequency phonon radiators and, briefly, to heat conduction from a solid to liquid helium.

2. Model Equations of Motion and Solutions: Phonon Transmission Coefficients

The model system considered here is shown schematically in Figure 1. Two linear harmonic chains are connected by a spring. Assume for simplicity that the equilibrium distance between any two adjacent masses is equal to a. Let u_j be the longitudinal displacement of mass j from its equilibrium position. The equations of motions for the u_j are

$$\begin{aligned}
\ddot{u}_j &= \omega_1^2 (u_{j+1} + u_{j-1} - 2u_j) && j \leqq -1 \\
\ddot{u}_0 &= \alpha_1^2 u_1 + \omega_1^2 u_{-1} - (\alpha_1^2 + \omega_1^2) u_0 \\
\ddot{u}_1 &= \omega_2^2 u_2 + \alpha_2^2 u_0 - (\alpha_2^2 + \omega_2^2) u_1 \\
\ddot{u}_j &= \omega_2^2 (u_{j+1} + u_{j-1} - 2u_j) && j \geqq 2 \qquad (1)
\end{aligned}$$

with

$$\begin{aligned}
\omega_i^2 &= f_i/m_i \\
\alpha_i^2 &= f_3/m_i, \qquad i = 1, 2. \qquad (2)
\end{aligned}$$

We are interested in traveling-wave solutions to Equations (1), i.e. in solutions of the form

$$\begin{aligned}
u_j &= \exp i(jk_2 a + \gamma t) + b \exp i(-jk_2 a + \gamma t) && j \geqq 1 \\
u_j &= c \exp i(jk_1 a + \beta t) && j \leqq 0. \qquad (3)
\end{aligned}$$

These represent an incoming wave in medium 2, which is partially reflected and partially transmitted to medium 1. For Equations (3) to be solutions of (1), one must have $\beta = \gamma$. On the other hand, because of the first and fourth equation in (1),

$$\begin{aligned}
\beta &= 2\omega_1 \sin \tfrac{1}{2} k_1 a \\
\gamma &= 2\omega_2 \sin \tfrac{1}{2} k_2 a. \qquad (4)
\end{aligned}$$

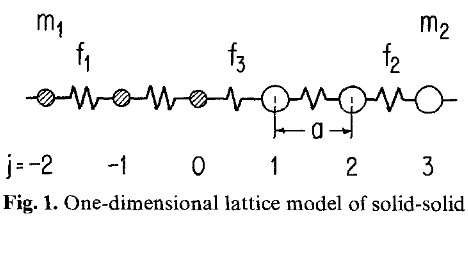

Fig. 1. One-dimensional lattice model of solid-solid interface

Hence

$$\omega_1 \sin \tfrac{1}{2} k_1 a = \omega_2 \sin \tfrac{1}{2} k_2 a \qquad (5)$$

which determines k_1 as a function of k_2. After inserting Equations (3) into the second and third of Equations (1), one obtains

$$\begin{aligned}
&c\left(\exp ik_1 a + \frac{f_3}{f_1} - 1\right) - b\frac{f_3}{f_1}\exp(-ik_2 a) = \frac{f_3}{f_1}\exp ik_2 a \\
&c\frac{f_3}{f_2} - b\left(1 + \left[\frac{f_3}{f_2} - 1\right]\exp(-ik_2 a)\right) \\
&= 1 + \left[\frac{f_3}{f_2} - 1\right]\exp ik_2 a. \qquad (6)
\end{aligned}$$

It is straightforward to solve these equations for b and c. In calculating the heat flux across the interface we will need $|b|^2$ and $|c|^2$. Let f_{31} and f_{32} be defined by

$$f_{3i} = f_3/f_i \qquad i = 1, 2. \qquad (7)$$

One then finds that $|b|^2$ and $|c|^2$ can be expressed as

$$|b|^2 = b_n/d \qquad |c|^2 = c_n/d \qquad (8)$$

with

$$\begin{aligned}
b_n &= (f_{31} + f_{32} - 1)^2 + 1 + (f_{31} - 1)^2 + (f_{32} - 1)^2 \\
&+ 2[\cos k_1 a][f_{31} - 1 - (f_{32} - 1)(f_{31} + f_{32} - 1)] \\
&+ 2[\cos k_2 a][f_{32} - 1 - (f_{31} - 1)(f_{31} + f_{32} - 1)] \\
&+ 2[\cos(k_1 + k_2)a](f_{31} - 1)(f_{32} - 1) - 2[\cos(k_1 - k_2)a] \\
&\cdot (f_{31} + f_{32} - 1) \qquad (9\text{a})
\end{aligned}$$

$$c_n = 4 f_{31}^2 \sin^2 k_2 a \qquad (9\text{b})$$

$$\begin{aligned}
d &= (f_{31} + f_{32} - 1)^2 + 1 + (f_{31} - 1)^2 + (f_{32} - 1)^2 \\
&+ 2[\cos k_1 a][f_{31} - 1 - (f_{32} - 1)(f_{31} + f_{32} - 1)] \\
&+ 2[\cos k_2 a][f_{32} - 1 - (f_{31} - 1)(f_{31} + f_{32} - 1)] \\
&- 2[\cos(k_1 + k_2)a](f_{31} + f_{32} - 1) + 2[\cos(k_1 - k_2)a] \\
&\cdot (f_{31} - 1)(f_{32} - 1). \qquad (9\text{c})
\end{aligned}$$

Equations (9) together with Equation (5) furnish a complete description, within our model, of the scattering of an elastic wave at an interface as a function of wave vector.

The consistency of the expressions given for $|b|^2$ and $|c|^2$ can be checked by looking at the continuum limit and at energy conservation. In the continuum theory of acoustics it is well known [12] that at an interface between two media which do not sustain shear stress, the reflection and transmission coefficients for a normally incident wave are given by

$$b^{(c)} = \frac{\rho_1 v_1 - \rho_2 v_2}{\rho_1 v_1 + \rho_2 v_2}, \qquad c^{(c)} = \frac{2\rho_2 v_2}{\rho_1 v_1 + \rho_2 v_2} \qquad (10)$$

where ρ_i and v_i stand for the mass density and the velocity of sound respectively in medium i. On the other hand, on expanding Equations (9) to order $(k_2 a)^2$ and using Equation (5) one finds

$$\lim_{k_2\to 0} |c| = \frac{2}{1+\left(\frac{m_1 f_1}{m_2 f_2}\right)^{\frac{1}{2}}}$$

$$\lim_{k_2\to 0} |b| = \frac{1-\left(\frac{m_1 f_1}{m_2 f_2}\right)^{\frac{1}{2}}}{1+\left(\frac{m_1 f_1}{m_2 f_2}\right)^{\frac{1}{2}}}. \tag{11}$$

Hence in the continuum limit Equations (9) reduce to the proper expressions if we make the obvious identification $\rho_i v_i \leftrightarrow (m_i f_i)^{\frac{1}{2}}$. Furthermore, it is easy to show that for all k_2

$$|b(k_2)|^2 + \frac{m_1 v_1(k_1)}{m_2 v_2(k_2)} |c(k_2)|^2 = 1 \tag{12}$$

if $v_1(k_1) = d\beta/dk_1$ and $v_2(k_2) = d\gamma/dk_2$, i.e. if the $v_i(k_i)$ are the proper group velocities, k_1 being determined by k_2 through Equation (5).

Figures 2 to 5 give some examples for the dependence of transmission coefficients on wave vector. Figure 2 shows curves for $|c(k_2)|$, the absolute value of the amplitude transmission coefficient, and Figure 3 shows corresponding curves for the power transmission coefficient $c_p(k_2)$, which is defined as

$$c_p(k_2) = \frac{m_1 v_1(k_1)}{m_2 v_2(k_2)} |c(k_2)|^2 \tag{13}$$

(cf. Eq. (12)). Note first that the continuum values may or may not be good approximations for $|c(k_2)|$ and $c_p(k_2)$ at finite k_2, depending on the values of the

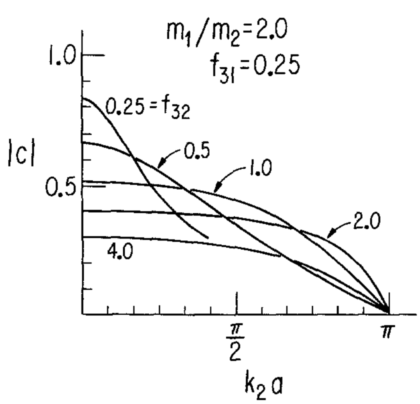

Fig. 2. Absolute value of amplitude transmission coefficient for a phonon going from medium 2 to medium 1 as a function of phonon wave vector. Total reflexion occurs in the case where $f_{32}=0.25$

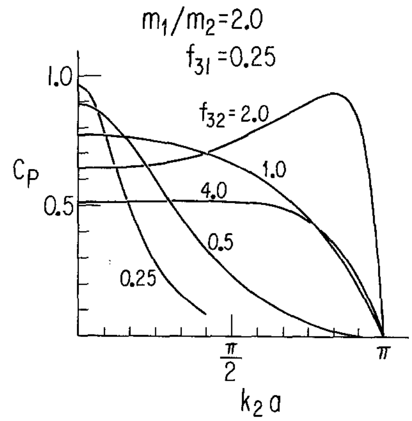

Fig. 3. Power transmission coefficient for a phonon going from medium 2 to medium 1 as a function of phonon wave vector. Note resonance phenomenon when $f_{32}=2.0$ and total reflexion when $f_{32}=0.25$

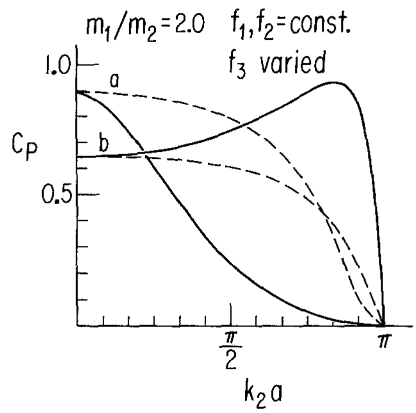

Fig. 4. Dependence of phonon power transmission coefficient on interface spring constant f_3. Curves a: $f_1=2f_2$; b: $f_1=8f_2$; ———: $f_3=0.25 f_1$; -----: $f_3=0.5 f_1$

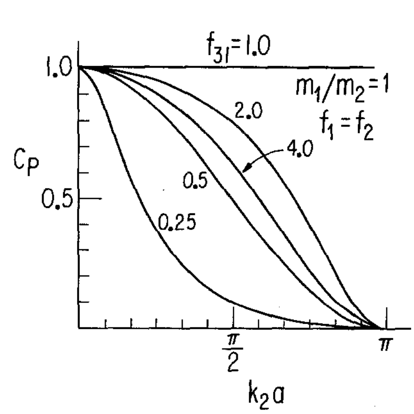

Fig. 5. Dependence of phonon power transmission coefficient on interface spring constant f_3 for a one-dimensional grain boundary

model parameters. In addition, if $\omega_2 > \omega_1$, then k_1 becomes complex as soon as k_2 increase above some limiting value (cf. Eq. (5)), and the incoming wave is totally reflected. Such is the case for the curves with $f_{32}=0.25$ in Figures 2 and 3. (In the continuum theory, total reflexion can only occur at oblique incidence [12]). Furthermore, although $c_p(k_2)$ in general decreases with increasing k_2, it is possible for $c_p(k_2)$ to exhibit some kind of resonant behavior (cf. curve with $f_{32}=2.0$ in Fig. 3). The importance of the interface bond is illustrated further in Figures 4 and 5 where the form of $c_p(k_2)$ can be seen to depend strongly on the interface spring constant f_3.

With a view on studying heat transfer across the interface, we have concentrated so far on traveling-wave solutions to Equations (1). However, for some model parameter values there exists also a solution to Equations (1) of the form

$$\begin{aligned} u_j &= A \exp i(jk_2 a - \beta t) \exp(-|j| l_2 a) \qquad j \geqq 1 \\ u_j &= B \exp i(jk_1 a - \beta t) \exp(-|j| l_1 a) \qquad j \leqq 0 \end{aligned} \tag{14}$$

corresponding to a local mode. The simplest situation is that of a one-dimensional crystal with a grain boundary: $m_1 = m_2$, $f_1 = f_2 \neq f_3$. It is then straightforward to show, by inserting Equations (14) into Equations (1), that there is a local mode if $f_3 > f_1$. This local mode splits off at the top of the band since

$$\beta^2 = 4\omega_1^2 (2 f_1/f_3 - (f_1/f_3)^2)^{-1} > 4\omega_1^2. \tag{15}$$

The situation just described is the dual analogue to a linear chain with a single impurity, where a local mode exists if the impurity atom is lighter than the other atoms [13]. In the slightly more complicated case where $m_1 \neq m_2$ and $f_1 = f_3 \neq f_2$ one finds a local mode with

$$\beta^2 = \frac{1}{m_1 m_2} \frac{(f_1 m_1 - f_2 m_2)^2}{(f_1 - f_2)(m_1 - m_2)} \tag{16}$$

if $f_1 > f_2$, $m_1 > m_2$ and $f_1/f_2 + m_2/m_1 > 2$.

Equation (16) was also derived previously by Hori et al. [14] using a Green's function method.

3. Heat Flux across Interface: Thermal Boundary Resistance

Let T_1 and T_2 be the temperatures on either side of the interface. Then one can write down the following, within our model exact expression for the heat flux due to phonons from medium 2 to medium 1.

$$q_2 = \tfrac{1}{2} \int_0^{2\omega_2} [\exp(\hbar\omega/k_B T_2) - 1]^{-1} g_2(\omega) \hbar\omega v_2(\omega) \cdot c_{p2}(\omega) d\omega. \tag{17}$$

In Equation (17) $g_2(\omega)$ is the exact $1D$ density of states [13], $v_2(\omega)$ is the group velocity for phonons, and $c_{p2}(\omega)$ is the power transmission coefficient from medium 2 to medium 1. The factor $\frac{1}{2}$ occurs because only half the phonons within the Brillouin zone move towards the interface. Equation (17) will be compared to the approximate expression

$$q_2^{(c)} = \tfrac{1}{2} \int_0^{\omega_D} [\exp(\hbar\omega/k_B T_2) - 1]^{-1} g_2^{(D)}(\omega) \hbar\omega \cdot v_2 \Gamma^{(c)} d\omega \tag{18}$$

where $g_2^{(D)}(\omega)$ stands for the Debye $1D$ density of states [13], v_2 for the usual velocity of sound, and $\Gamma^{(c)}$ for the continuum power transmission coefficient.

From Equation (11)

$$\Gamma^{(c)} = \frac{4(m_1 f_1 m_2 f_2)^{\frac{1}{2}}}{[(m_1 f_1)^{\frac{1}{2}} + (m_2 f_2)^{\frac{1}{2}}]^2}. \tag{19}$$

Let us also introduce an average transmission coefficient $\Gamma_2(T_2)$ by

$$v_2 \Gamma_2(T_2) = \frac{\int_0^{2\omega_2} [\exp(\hbar\omega/k_B T_2) - 1]^{-1} g_2(\omega) \hbar\omega v_2(\omega) c_{p2}(\omega) d\omega}{\int_0^{2\omega_2} [\exp(\hbar\omega/k_B T_2) - 1]^{-1} g_2(\omega) \hbar\omega d\omega}. \tag{20}$$

The denominator in Equation (20) is equal to the energy density $\varepsilon_2(T_2)$. This allows Equation (17) to be rewritten in the suggestive form [16]

$$q_2 = \tfrac{1}{2} \varepsilon_2(T_2) v_2 \Gamma_2(T_2). \tag{21}$$

$\Gamma_2(T_2)$ is particularly useful for a comparison of the exact and the continuum treatment because

$$\lim_{T_2 \to 0} \Gamma_2(T_2) = \Gamma^{(c)}.$$

For the net heat flux q_{21} across the interface, from Equation (21),

$$q_{21} = \tfrac{1}{2} \varepsilon_2(T_2) v_2 \Gamma_2(T_2) - \tfrac{1}{2} \varepsilon_1(T_1) v_1 \Gamma_1(T_1). \tag{22}$$

If $T_2 - T_1 \ll T_2$, then q_{21} is proportional to $T_2 - T_1$. This means that heat flux from one medium to the other requires a finite temperature jump at the interface.

The quantity $(T_2 - T_1)/q_{21}$ is called thermal boundary resistance.

Figures 6 and 7 present a numerical comparison between exact and continuum results for heat flux across the $1D$ analogue of a $Ni-Al_2O_3$ interface. In order for the values of the model parameters to be representative of real materials, m_2/m_1 was set equal to ρ_2/ρ_1, and f_2/f_1 was determined by setting ω_2/ω_1 equal to θ_{D2}/θ_{D1}, the ratio of Debye temperatures. (In

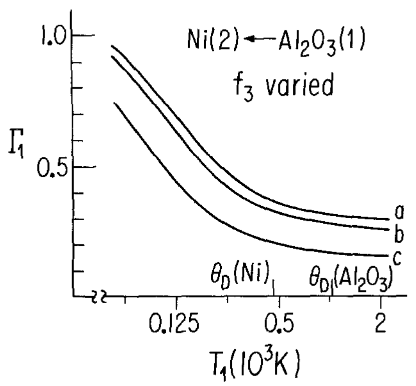

Fig. 6. Average transmission coefficient as a function of temperature. The model parameters are chosen such as to represent a one-dimensional analogue of a Ni (medium 2)$-Al_2O_3$ (medium 1) interface: $m_1/m_2=0.45$, $f_1/f_2=2.3$, f_3 variable. Curves a: $f_3=(f_1 f_2)^{\frac{1}{2}}$; b: $f_3=4(f_1 f_2)^{\frac{1}{2}}$; c: $f_3=0.25(f_1 f_2)^{\frac{1}{2}}$. Heat flow is from Al_2O_3 to Ni. Thermal matching is optimal for $f_3=(f_1 f_2)^{\frac{1}{2}}$

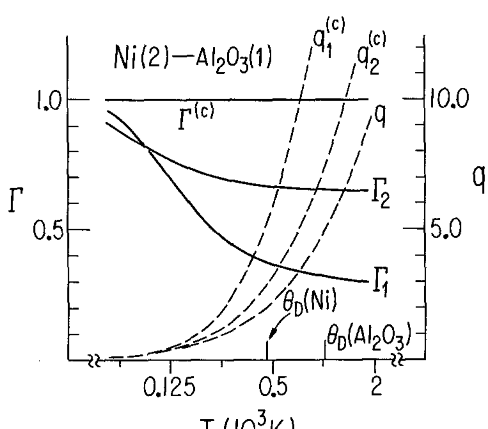

Fig. 7. Comparison of exact and continuum results for average transmission coefficient Γ and heat flux q (arbitrary units). Same values for model parameters as in Figure 6, with $f_3=(f_1 f_2)^{\frac{1}{2}}$. $q_1^{(c)}$ denotes continuum heat flux from medium 1 to medium 2. Note that $q_1^{(c)}(T) \neq q_2^{(c)}(T)$ in contradiction to thermodynamics

one dimension, $\omega \propto \theta_D \propto v$ [13].) However, the qualitative aspects of our results do not depend significantly on the precise values of the model parameters. Figure 6 shows that the average transmission coefficient $\Gamma(T)$, calculated from Equation (20), generally decreases with increasing T such that $\Gamma^{(c)}$ will not be a good approximation to $\Gamma(T)$ for $T \gtrsim 0.1\,\theta_D$. In addition, Figure 6 demonstrates again the importance of the interface bond: $\Gamma(T)$ depends appreciably on f_3, and heat transfer across the interface is optimal if $f_3=(f_1 f_2)^{\frac{1}{2}}$. Figure 7 illustrates the correspondence between $q(T)$ and $\Gamma(T)$. Note also that the continuum treatment violates thermodynamics since it gives $q_{21}^{(c)} \neq 0$ for $T_2=T_1$. This is in contrast to the exact treatment, for which $q_{21}=0$ if $T_2=T_1$. From Figures 6 and 7 we further conclude that $\Gamma(T)$ is not a very strong function of T at high temperature. At the same time $\varepsilon(T)=k_B T$ so that at high temperature q_{21} is again very nearly proportional to T_2-T_1.

4. Applications

Before dealing with specific applications, we shall discuss to what extent the results of our one-dimensional model calculation apply to a three-dimensional interface in general. In real solids, propagating elastic waves must be described not only by their wave vector but also by their polarization. At a $3D$ interface, longitudinal and transverse waves are coupled to each other in a complicated manner [7]. The dispersion relation and the density of states also differ considerably between one and three dimensions [13]. In addition, very little is known about the structure of a solid-solid interface on an atomic scale. Most of the information available comes from experiments on the adhesive properties of thin films deposited on a substrate [15]. Although such experiments are notoriously difficult to interpret, it is clear that the strength of the film-substrate bond can vary within a wide range, depending on the conditions under which the film was formed. Also, except possibly for epitaxially grown films, the distance over which the elastic properties at the interface change appreciably will probably be of the order of several lattice constants.

In view of all these problems, it is essential to realize that the important qualitative aspects of the results of our $1D$ calculation are due basically to a dimensional effect: Phonons are scattered strongly by a lattice defect if their wavelength is comparable to the dimensions of the defect. In our case the defect is the interface, whose thickness is of the order of a few lattice constants. Hence interface scattering is strongest for short-wavelength phonons, and such phonons are present in higher proportion at high temperatures. In particular, Equation (22) for the net heat flux across the interface carries over to the $3D$ case, with $\Gamma(T)$ being interpreted as a transmission coefficient properly averaged over all phonon branches [16]. From the above arguments, this $\Gamma(T)$ can also be expected to decrease with increasing temperature.

4.1. Heat Dissipation in Catalysts

Catalysts for many industrial processes consist of small transition-metal particles finely dispersed on a porous insulating substrate. Chemical reactions occurring on these metal particles often involve excited intermediates, and the processes by which this excitation energy is dissipated are crucial in determining

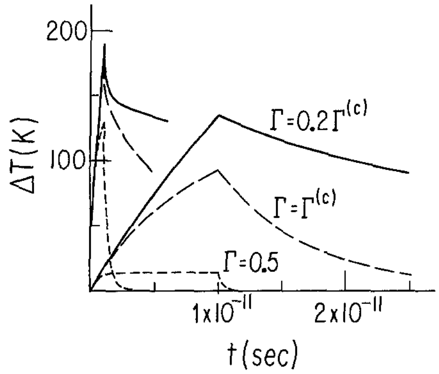

Fig. 8. Transient heating of a Pt catalyst particle (diameter 50 Å), sitting on an Al_2O_3 substrate, when subjected to a heat pulse (30 kcal/mole, 10^{-12} or 10^{-11} s duration) from a chemical reaction. $\Gamma=0.5$ corresponds to perfect thermal matching between particle and substrate. $\Gamma^{(c)}=0.06$ (cf. Ref. 16). $\Gamma(T)=0.2\,\Gamma^{(c)}$ should be a realistic estimate at the temperatures involved

the operation of a catalyst [16, 17]. Part of this excitation energy will be released to the catalyst in the form of short, fairly intense pulses of heat. Because of the thermal boundary resistance between the catalyst particles and their support, these heat pulses may lead to large local temperature fluctuations and thus affect chemical reaction rates as well as the stability of the catalyst [16, 17].

Figure 8 shows the temperature rise of a medium-sized (50 Å) Pt particle on an Al_2O_3 substrate subjected to a heat pulse (30 kcal/mole) from a moderately exothermic reaction. (For computational details see Ref. 16). The value of the phonon transmission coefficient Γ at the particle-substrate interface is clearly crucial in determining the temperature rise and subsequent cooling of the catalyst particle. Note that at the temperatures involved $\Gamma^{(c)}$ is not a good approximation to $\Gamma(T)$. Also, for smaller particles heating turns out to be even more severe [16].

4.2. High-Frequency Phonon Radiators

In recent years it has become possible to generate and perform experiments with phonons of very high frequency [2]. Superconducting tunnel junctions are able to produce fairly monochromatic phonons with frequencies up to $\sim 10^{12}\,s^{-1}$ ($\lambda \sim 50$ Å). From heat pulse techniques using thin film radiators phonons with frequencies up to $10^{13}\,s^{-1}$ ($\lambda \sim 5$ Å) are available. The propagation properties of these high-frequency phonons are a subject of interest in itself, but such phonons are also used e.g. as probes for electronic relaxation processes [2]. Our results are pertinent to such experiments since they all involve transmission of short-wavelength phonons across a metal-insulator interface.

Superconducting tunnel junctions, whether used as phonon generators or detectors, typically consist of a metal film (e.g. Al) which is separated by an insulating layer (e.g. SiO_2) from the material (e.g. Cu) in which phonon propagation is to be studied [2, 18]. Clearly the efficiency and spectral characteristics of the generator junction and the sensitivity of the detector junction both depend on the phonon transmission coefficient across the SiO_2/Cu interface. Our results suggest that at the phonon frequencies in question, the continuum value is probably not a good approximation to that transmission coefficient. Furthermore, in order to obtain a bulk scattering length for the phonons, one has to take into account scattering by grain boundaries. The presence of grains of different orientation not only leads to an effective average sound velocity for the phonons [18], but the grain boundaries themselves may give rise to considerable phonon scattering (cf. Fig. 5). Indeed phonon attenuation is found to be much larger in films with small grains [18].

As regards heat pulse phonon radiators, it should be noted that the continuum acoustic mismatch theory predicts well the radiation characteristics at low radiation temperatures. However, at higher radiation temperatures the measured phonon flux is usually smaller than predicted by a factor of 2 to 5 [3–5]. But this is precisely what would be expected from our results on the form of the transmission coefficient $\Gamma(T)$. In addition, the importance of the atomic structure of the film-substrate interface is evidenced by the fact that radiators involving a Pb film were in general more efficient than predicted unless special precautions were taken to keep the substrate free of contaminants during film evaporation [3–5].

4.3. Kapitza Resistance

As noted in the introduction, a modified continuum theory of thermal boundary resistance is able to describe heat conduction between liquid helium and a solid at temperatures below 0.1 K [1, 10, 11]. However, it is not clear yet what mechanisms of heat transfer will give rise to the observed increase above 0.2 K and to the possible maximum around 6 K of the phonon transmission coefficient [1, 19, 20]. Heat transfer at these temperatures may at least in part be of gaskinetic origin [4, 21].

Our study, although focussing primarily on solid-solid interfaces, suggests that even in the case of a liquid helium-solid interface, the atomic structure of the surface of the solid may not be negligible. An inspection of the phonon dispersion relation in liquid helium [22] reveals that at 1 K an appreciable number of phonons with $\lambda \lesssim 100$ Å are present. On the other hand, it is well established from studies of the structure of single-crystal surfaces [23–25] that such surfaces are disordered on a scale of 100 Å, even after being electropolished, and are covered by one or more monolayers of impurities (e.g. carbon) unless they are carefully cleaned and annealed in *ultra-high vacuum.* Hence a continuum theory of Kapitza resistance may be inadequate, and in comparing experiments with each other and with theory careful attention should be paid to the state of the solid surface. There is experimental evidence showing that in some instances surface preparation does affect the efficiency of heat transfer between a solid and liquid helium [1, 11].

5. Conclusion

The main results of this paper have been a calculation, within a $1D$ lattice model, of transmission coefficients for phonons across a solid-solid interface as a function of phonon wavelength, and a discussion, with applications, of thermal boundary resistance at high temperature in terms of an average temperature-dependent phonon transmission coefficient.

These results suggest future research in two directions. First, it would be interesting to check the conclusions arrived at here with a calculation using an analogous $3D$ model of a solid-solid interface. Second, experiments on thermal boundary resistance should be performed in which the atomic structure of the interface is controlled as carefully as possible. One intriguing prospect of such experiments is the development of composite thin films which transmit an unusually large flux of phonons or only phonons within a narrow frequency range.

I thank B. Bell for reading the manuscript. This work has been supported in part by ARPA ONR grant No N00014-75-C-1107.

References

1. Challis, L.J.: J. Phys. C: Sol. State Phys. **7**, 481 (1974)
2. Renk, K.F.: in Festkörperprobleme XII, edited by O. Madelung. New York-Braunschweig: Pergamon and Vieweg 1972
3. Herth, P., Weis, O.: Z. Angew. Phys. **29**, 101 (1970)
4. Kappus, W., Weis, O.: J. Appl. Phys. **44**, 1947 (1973)
5. Cheeke, J.D.N., Hebral, B., Martinon, C.: J. Phys. (Paris) **34**, 257 (1973)
6. Khalatnikov, I.M.: Introduction to the Theory of Superfluidity. New York: Benjamin 1965
7. Little, W.A.: Can. J. Phys. **37**, 334 (1959)
8. Neeper, D.A., Dillinger, J.R.: Phys. Rev. **135**, A1028 (1963)
9. Wigmore, J.K.: Phys. Rev. B**5**, 700 (1972)
10. Haug, H., Weiss, K.: Phys. Lett. **40**A, 19 (1972)
11. Peterson, R.E., Anderson, A.C.: J. Low Temp. Phys. **11**, 639 (1973)
12. Kinsler, L.E., Frey, A.R.: Fundamentals of Acoustics. New York: Wiley 1950
13. Donovan, B., Angress, J.F.: Lattice Vibrations. London: Chapman and Hall 1971
14. Hori, J., Ono, M., Ogura, M., Wada, K.: in Proc. Int. Conf. on Phonons, Rennes 1971, edited by M.A. Nusimovici. Paris: Flammarion 1971
15. Chapman, B.N.: J. Vac. Sci. Technol. **11**, 106 (1974)
16. Steinbrüchel, Ch., Schmidt, L.D.: Surf. Sci. **40**, 693 (1973)
17. Steinbrüchel, Ch., Schmidt, L.D.: J. Vac. Sci. Technol. **11**, 267 (1974)
18. Long, A.R.: J. Phys. F: Metal Phys. **3**, 2023, 2040 (1973)
19. Guo, C.-J., Maris, H.J.: Phys. Rev. A**10**, 960 (1974)
20. Swanenburg, T.J.B., Wolter, J.: Phys. Rev. Lett. **33**, 882 (1974)
21. Sluckin, T.J.: Phys. Lett. **53**A, 390 (1975)
22. Woods, A.D.B., Cowley, R.A.: Can. J. Phys. **49**, 177 (1971)
23. Bauer, E.: in Interactions on Metal Surfaces, edited by R. Gomer. New York-Heidelberg-Berlin: Springer 1975
24. Somorjai, G.A.: Principles of Surface Chemistry. Englewood Cliffs: Prentice-Hall 1972
25. Blakely, J.M.: Introduction to the Properties of Crystal Surfaces. Oxford-New York: Pergamon 1973

Ch. Steinbrüchel
The James Franck Institute
The University of Chicago
Chicago, Illinois 60637
USA